JOURNAL OF MATERIALS SCIENCE 21 (1986) 3933–3940

Characterization and thermal behaviour of gel grown mixed rare-earth (Didymium) tartrate crystals

P. N. KOTRU, K. K. RAINA, M. L. KOUL*
*Department of Physics and *Department of Chemistry, University of Jammu, Jammu 180001, India*

Spherulites, crystal aggregates and platelets of $Di_2^{\dagger}(C_4H_4O_6)_3 \cdot 5H_2O$ mixed crystals were grown in gel using the single tube diffusion method. The material was characterized by using different techniques such as chemical analysis, EDAX, X-ray and electron diffraction, infrared and mass spectroscopy. The thermal behaviour of the material was studied using differential thermal analysis, DTG, thermogravimetric analysis and differential scanning calorimetry. The material is thermally unstable and starts decomposing at 50° C. Thermal analysis results indicate the application of the contracting cylindrical kinetic model for the solid state reactions involved in the decomposition process. The values of kinetic parameters, e.g. order of reaction, activation energy and frequency factor are worked out. The implications are discussed.

1. Introduction

There has been an increasing trend over the recent years, beginning from the 1960s, to grow and explore the properties of mixed crystals. The growth and characterization of cation iron garnets [1–3], rare-earth Na–Mo sheelites [4], alkali halides [5–8], certain ferrites [9, 10] and II–IV compounds [11] involving high temperature growth techniques and calcium–strontium tartrate [12–15] using low temperature solution growth (gel method) indicates the growing interest in this flourishing new culture. Growth of mixed crystals of various compositions is a fast growing field of research because of the great need of such crystals for several applications. Crystal growth in gels offers itself as a simple and inexpensive method for useful experiments on the growth of mixed crystals for scientific investigations. Compounds of tartaric acid find several practical applications in science and technology [16]. Since the compounds of rare-earth tartrates are practically insoluble in water and decompose at fairly low temperatures [17–19] the gel technique is the most appropriate one for their growth. Kotru *et al.* [20–23] have successfully employed the gel technique for the growth of pure rare-earth (R = Gd [20]; La [21]; Nd and Dy [22]) tartrate crystals. The gel technique has also been successfully employed for the growth of mixed crystals of didymium tartrate crystals [23].

Characterization is a key to information, making identification and understanding of characteristic properties of the grown material possible. The data on characteristics of rare-earth tartrates being extremely limited, it is difficult to identify and understand their characteristic properties straightaway. In this laboratory, some pure rare-earth tartrate crystals grown in silica gels have been characterized [20–22]. In this paper, the authors report results obtained on characterization of mixed crystals of didymium tartrate crystals by chemical analysis, EDAX, X-ray and electron diffraction, IR and mass spectroscopic techniques and thermal analysis. The study provides the data on vital characteristics which enables one to distinguish the mixed crystals (say $(R'R'')_2(C_4H_4O_6)_3 xH_2O$ where R′ and R″ are two different rare-earth ions) from the pure ones (say $R'_2(C_4H_4O_6)_3 \cdot xH_2O$ and $R''_2(C_4H_4O_6)_3 \cdot xH_2O$).

2. Experimental procedure

Mixed crystals of rare-earth (didymium) tartrate crystals were grown by the single tube single gel technique, as described by Kotru *et al.* [23]. In order that the stoichiometry of the grown crystals is established, conventional physical and chemical methods were used. Carbon and hydrogen was estimated by employing carbon–hydrogen analysing equipment. Metal was estimated by employing conventional chemical techniques. Qualitative elemental analysis was carried out by employing an EDAX attachment of an SEM (Cambridge stereoscan type 7313), after coating the material with gold. Philips X-ray powder diffractometer model PW1350 with nickel filtered Cu$K\alpha$ radiation (30 kV, 15 mA) was used to obtain powder diffraction patterns. The instrument was set for a scanning speed of 2° in 2θ min^{-1}, and rate meter and chart speed were maintained constant. The electron diffraction was recorded on a TEM, model AE1 TEM-802 made in the UK. The mass spectrum was recorded by mass spectrometer model JMS-300, using 70 eV electron bombardment for ionization. The IR spectrum ranging from 200 to 4000 cm^{-1} was recorded on an SP 2000 IR spectrophotometer manufactured

†Didymium (Di) is a mixture of La, Nd, Pr and Sm.

0022–2461/86 $03.00 + .12

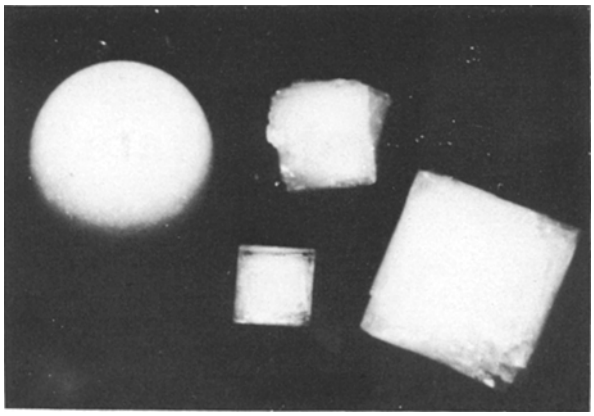

Figure 1 Spherulitic and platelets mixed rare earth crystals of $Di_2(C_4H_4O_6)_3 \cdot 5H_2O$ grown in silica gel ($\times 60$).

by Pye Unicam, UK, using the KBr pellet technique. The thermal behaviour of the material was registered in simultaneously recorded thermogravimetric (TG), DTG and differential thermal analysis (DTA) curves, using a Pauli-Pauli-Erday MOM. Derivatograph, model OD 103 made in Hungary. 200 mg of the sample were taken and the heating rate was maintained at $10° min^{-1}$ in air. Differential scanning calorimetry (DSC) curves were obtained on a Mettler thermal analyser between 60 and 540° C in ambient atmosphere at a heating rate of $10° C min^{-1}$ using base line type 1 and plot mode 1. Kinetic parameters of solid state reactions such as activation energy, order of reaction and frequency factor were determined from thermal analysis by using different equations, as described in the relevant places in the text.

3. Results and discussion

The silica gel property of controlled diffusion in the system $Di_2(NO_3)_3$–Na_2SiO_3–$C_4H_6O_6$ leads to the growth of mixed crystals of didymium tartrate, assuming single crystal platelet, crystal aggregate and spherulitic morphologies. The crystals grown in such a system are shown in Fig. 1. The charaterization and thermal behaviour of the grown material is described and discussed as follows.

3.1. Characterization

3.1.1. Chemical analysis/EDAX

The stoichiometry of didymium tartrate crystals was established by metal and carbon–hydrogen analysis. The results of the analysis as recorded in Table I suggest the material to have 5 waters of hydration; the chemical composition of the material having thus been established as $Di_2(C_4H_4O_6)_3 \cdot 5H_2O$. Association of five waters of hydration with the mixed crystals is further supported by the thermogram (TG) whose

TABLE I Chemical analysis of $Di_2(C_4H_4O_6)_3 \cdot 5H_2O$ (MW ≈ 819)

Element	Composition (%)	
	Theoretical	Measured
C	17.58	16.9
H	2.68	3.2
Di	34.79	36.45

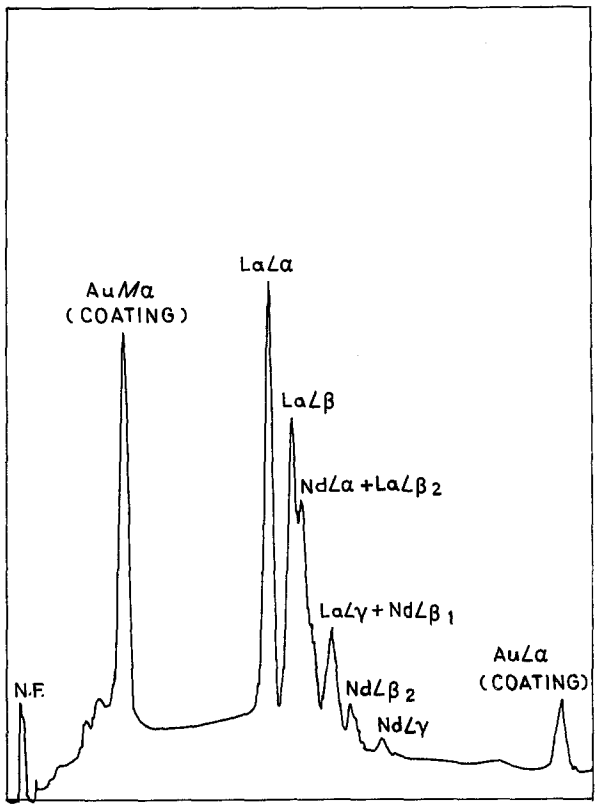

Figure 2 EDAX trace showing prominent peaks of La and Nd in didymium tartrate.

details follow further in the text. In the TG, a mass loss of 57.5% results in the formation of Di_2O_3. Knowing the initial mass of the material and the mass loss that follows on heating, stoichiometry of the material is worked out which is in complete agreement with that obtained from chemical analysis.

Qualitative elemental analysis performed on application of the EDAX reveal prominent peaks due to presence of lanthanum and neodymium (Fig. 2). The peaks of La and Nd are quite conspicuous, considering the fact that their concentration in the material is quite high. The presence of Pr and Sm was also detected through counts on the screen but on account of their low concentration in the material, the corresponding peak heights were very low.

It is significant to note that the data on characterization of gel grown mixed didymium tartrate crystals is reported for the first time.

3.1.2. Electron and X-ray diffraction

In order to check the state of crystallinity of the grown mixed crystals and their response to electron radiation, electron diffraction patterns were recorded. The material behaves in much the same way as other single (pure) rare-earth tartrates [20–22]. The diffraction patterns change on examination under the TEM, the change being almost spontaneous. Figs 3a and b are the electron diffraction patterns recorded immediately on and after some time of loading the sample prepared from spherulitic crystals, respectively. The spotty diffraction pattern in Fig. 3a indicates polycrystallinity of the parent material (spherulites) which immediately change to a ring pattern characteristic of complete deterioration in the crystallinity of the material. The result suggests electron diffraction as the destructive

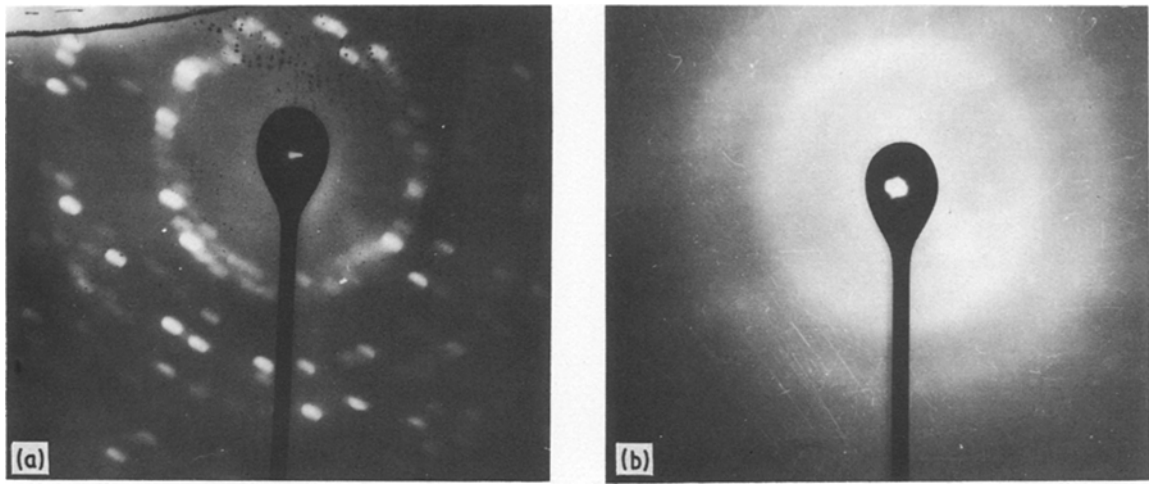

Figure 3 (a) Electron diffraction pattern recorded immediately on loading, (b) electron diffraction pattern recorded after some time of loading.

method for the material, making it irrelevant for any in depth study. The parent material on getting exposed to the electron radiation decomposes immediately. Hydrated materials are often confronted with this sort of problem [24]. Electron beam heating and the presence of waters of hydration seem to be the main causes behind this problem, as has also been reported for pure rare-earth tartrate crystals [20–22]. It may be noted that on account of almost spontaneous decomposition of the material while examination under TEM, it is difficult to say with certainty whether the diffraction pattern recorded immediately on loading belonged to the parent material or not.

The X-ray powder diffractogram recorded on the material is shown in Fig. 4. The trace (intensity against 2θ) indicates crystallinity of the material. The X-ray diffraction data compiled for $Di_2(C_4H_4O_6)_3 \cdot 5H_2O$ is given in Table II. The characteristic data on this material is reported here for the first time. To the best of authors knowledge, there is no X-ray diffraction data on these crystals available in the existing literature.

3.1.3. IR and mass spectroscopy

Fig. 5 is the characteristic IR spectrum of $Di_2(C_4H_4O_6)_3 \cdot 5H_2O$ in the range of 200 to 4000 cm^{-1}. Table III gives the details of band assignments. The broad and strong peak at 3400 cm^{-1} is due to water and OH stretching. A similar type of peak at 1615 cm^{-1} is due to C=O stretch. The strong peaks at 1420 and 1320 cm^{-1} are due to C–O sym. + δ (O–C=O) modes. There is a weak peak at 1287 cm^{-1} which may be attributed to OH in plane bending. The peaks 1140, 1065, 1075 and 945 cm^{-1} are attributed to δ CH + π CH, coordinated C–OH groups, δ CH, π CH and CO stretching and C–H stretch, respectively.

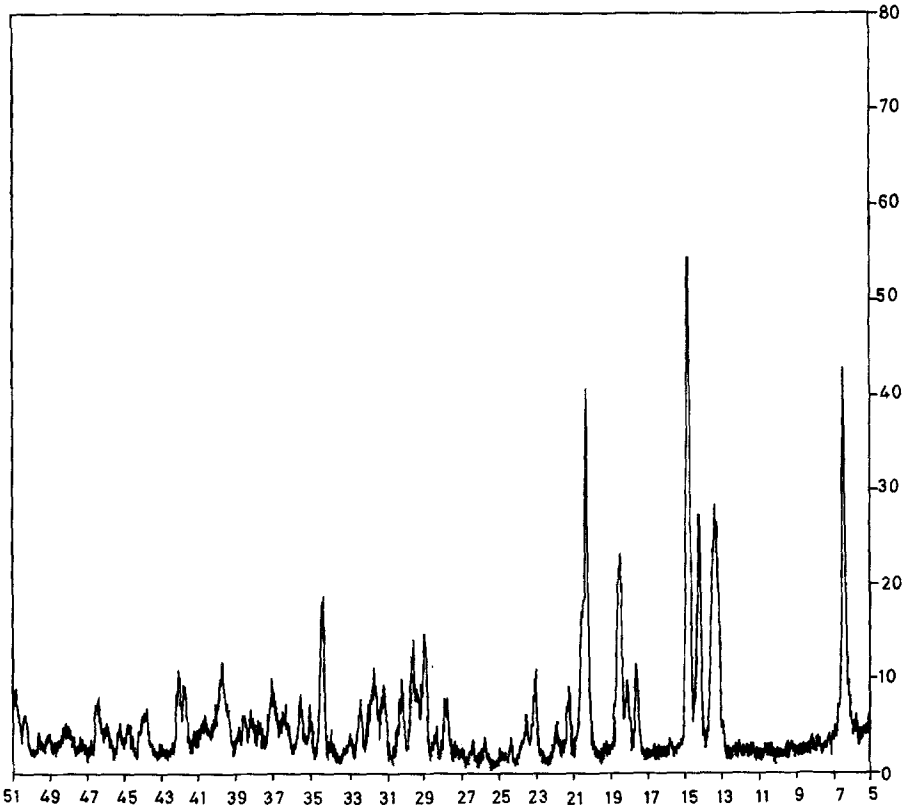

Figure 4 X-ray diffraction trace of $Di_2(C_4H_4O_6)_3 \cdot 5H_2O$.

TABLE II X-ray powder data

d (nm)	Intensity values
1.2998	41
0.65587	27
0.60669	24
0.57909	53
0.50390	9.0
0.47199	21
0.42908	38.5
0.38176	9
0.30582	12.5
0.30278	12
0.25881	17
0.22539	10

TABLE III IR band assignment for $Di_2(C_4H_4O_6)_3 \cdot 5H_2O$

Band (cm^{-1})	Assignment
1. 3400 (bs*)	ν (OH) water
2. 1615 (bs)	ν (C=O)
3. 1420 (bs)	ν (C–O) + δ (O–C=O)
4. 1320 (s†)	
5. 1287 (w)‡	δ (OH)
6. 1140 (s)	δ (C–H) + π (C–H)
7. 1065 (s)	Co-ordinated C–OH
8. 1075 (s)	δ (C–H), π (C–H) and ν (C=O)
9. 945 (s)	ν (C–H)

*bs = broad and strong.
†s = strong.
‡w = weak.

The IR spectrum thus shows all the bands expected from metal tartrate crystals with water of hydration.

Fig. 6 shows the mass spectrum of the penta-hydrated didymium tartrate. In this experiment 70 eV electron bombardment was used for ionization. The spectrum shows the base peak at M/E = 18 with the value of raw intensity equal to 912.8; the other prominent peaks are at M/E = 17, 28, 32. There is a weak peak at M/E = 149. The base peak at M/E = 18 is suggestive of the presence of water of hydration and the weak peak (with the value of raw intensity = 4.5) is suggested to be due to tartrate constituent of the original material, the molecule being

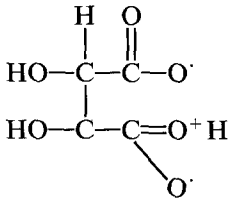

The mass fragmentography as obtained in case of $Di_2(C_4H_4O_6)_3 \cdot 5H_2O$ is recorded in Table IV. The mass spectrum (Fig. 6) and the compiled data in Table IV suggest the decomposition of the material and further supports the presence of water, carbon and oxygen as constituents of the material, which is most likely to happen on fragmentation of the tartrate and water of hydration associated with the parent material. Experiments were repeated in an attempt to capture the molecular ion along with the metal, had there been some volatility but without any success. The failure in detecting the molecular ion suggests that the molecule decomposes before it is captured.

The mass spectrometry supplements the findings from chemical analysis, IR and thermogravimetric analysis (described further in the text) regarding the chemical composition, besides suggesting the mass fragmentography at 70 eV of electron bombardment.

3.2. Thermal analysis

The results of electron diffraction and mass spectroscopy demonstrate the decomposition of the material at low energies. In this respect the material behaves in the same way as pure rare-earth tartrates [17–19]. It is, therefore, worthwhile to investigate the thermal behaviour of $Di_2(C_4H_4O_6)_3 \cdot 5H_2O$ in a greater detail, using DTA, DTG, TGA and DSC techniques.

Fig. 7 shows the thermograms, wherein TG, DTA and DTG are simultaneously recorded and Fig. 8 gives a DSC curve. Critical examination of the thermograms and the DSC make it clear that all transformations are associated with mass changes thereby suggesting that there is no physical transformation of the material. All changes in DTA and DSC correspond to the changes in TG. The results here rule out the possibility of mere physical change in the crystallinity of the intermediates during the process of decomposition.

The decomposition process of the $Di_2(C_4H_4O_6)_3 \cdot 5H_2O$ starts at 50° C up to which the material remains stable. The first stage of decomposition continues up

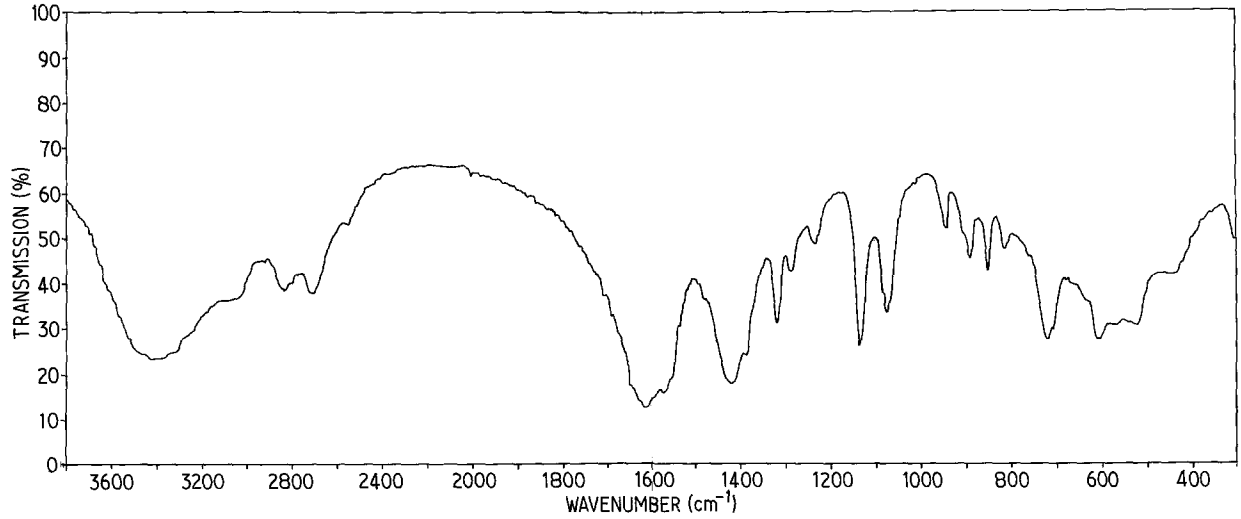

Figure 5 IR spectrum of $Di_2(C_4H_4O_6)_3 \cdot 5H_2O$.

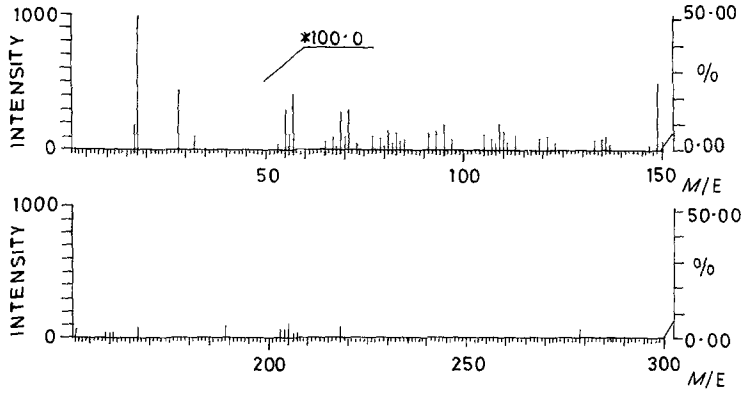

Figure 6 Mass spectrum of $Di_2(C_4H_4O_6)_3 \cdot 5H_2O$.

to 200° C leading to the formation of anhydrous didymium tartrate, which as is observed from TG remains stable up to 245° C. The second stage of decomposition starts at 235° C and is completed at 360° C, leading to the formation of didymium oxalate $[Di_2(C_2O_4)_3]$. This product remains stable up to the temperature of 380° C. In the third stage between 380 to 490° C the didymium oxalate decomposes to didymium carbonate. Finally, in the fourth stage between 490 to 760° C the didymium carbonate gets reduced to didymium oxide which remains stable on further heating. Table V gives a summarized analysis of different stages associated with the thermal decomposition of the material as observed in the TG of Fig. 7. The expected and observed mass losses at different steps are also shown in the table.

TABLE IV Mass spectrum data for $Di_2(C_4H_4O_6)_3 \cdot 5H_2O$

M/E	Raw intensity	Relative intensity	Sigma (%)
1.0	1.0	1.1	0.05
14.0	7.7	8.4	0.44
16.0	11.7	12.8	0.67
17.0	191.9	210.2	11.06
18.0	912.8	1000.0	52.63
19.0	11.0	12.1	0.63
20.0	2.0	2.2	0.11
27.0	1.4	1.5	0.08
28.0	416.5	456.2	24.01
29.0	5.8	6.4	0.33
32.0	98.3	107.7	5.67
39.0	1.0	1.2	0.06
40.0	7.0	7.7	0.40
41.0	3.1	3.4	0.18
43.0	4.4	4.8	0.25
44.0	17.8	19.5	1.03
45.0	1.1	1.3	0.06
55.0	2.8	3.1	0.16
56.0	1.1	1.2	0.06
57.0	3.9	4.3	0.22
67.0	1.0	1.1	0.06
69.0	2.7	3.0	0.16
70.0	1.0	1.1	0.05
71.0	2.8	3.1	0.16
77.0	1.0	1.1	0.05
81.0	1.5	1.6	0.08
83.0	1.3	1.4	0.07
91.0	1.2	1.3	0.07
93.0	1.4	1.5	0.08
95.0	1.8	2.0	0.10
105.0	1.2	1.3	0.07
109.0	1.9	2.1	0.11
110.0	1.4	1.5	0.08
113.0	1.1	1.2	0.06
119.0	0.9	1.0	0.05
121.0	1.1	1.2	0.06
136.0	1.0	1.1	0.06
149.0	4.5	5.0	0.26
205.0	1.0	1.2	0.06

The decomposition pattern is typical of a hydrated metal tartrate [25]. Analysis of thermal decomposition finally establishes the stoichiometry of the grown material. The stoichiometry is in complete agreement with the findings from chemical analysis. The study also gives a sound basis for an explanation (qualitative) of changes in the electron diffraction patterns while examined under TEM.

To understand the kinetics of solid state reactions leading to the decomposition of the material, the following equations were used in the calculation of activation energy E, order of reaction n and the frequency factor Z. This was done considering the first stage of decomposition only, as in the subsequent stages the sample characteristics can not be controlled. The following equations of Horowitz–Metzger [26], Piloyan–Novikova [27] and Coats–Redfern [28] were used for this purpose.

1. Horowitz–Metzger relation

$$\log\left[\frac{1-(1-\alpha)^{1-n}}{1-n}\right] = \frac{E}{2.303RT_m^2} \quad (1)$$

provided $n \neq 1$, i.e. $n = 1/2$, $1/4$, $2/3$, $1/3$ and $T - T_m = \theta$.

2. Piloyan–Novikova relation

$$\log(\alpha/T^2) = \log(ZR/\beta E) - E/2.303RT \quad (2)$$

for $\alpha = 0.05 - 0.5$. E is calculated from the slope of a straight line obtained on plotting $\log(\alpha/T^2)$ against $1/T$. The frequency factor Z is calculated from the intercept.

3. Coats–Redfern relation

$$\log[g(\alpha)/T^2] = \log[ZR/\beta E] - E/2.303RT \quad (3)$$

where $g(\alpha)$ turns out to be equal to $2[1-(1-\alpha)^{1/2}]$ in the present case, as it is this value of $g(\alpha)$ which gives the best linear fit in the graph of LHS against $1/T$. The plot yields a straight line from which energy of activation is calculated. The frequency factor Z is calculated from the intercept.

In these Relations 1 to 3 the parameters are as

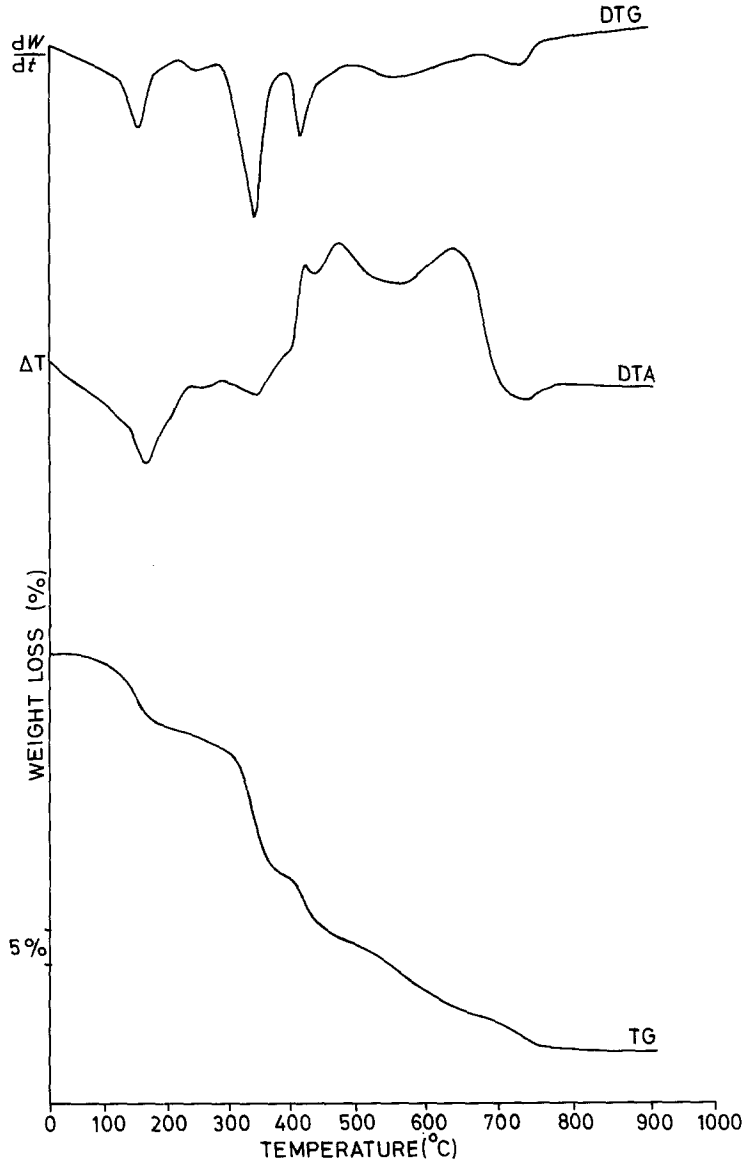

Figure 7 Thermogram showing DTA, DTG and TG curves of $Di_2(C_4H_4O_6)_3 \cdot 5H_2O$.

follows:

$$\alpha = \frac{\text{Weight loss up to particular temperature}}{\text{Total weight loss in the step}};$$

β = rate at which temperature increases;
T = temperature in Absolute scale;
Z = frequency factor; and
$T - T_m = \theta$, where T_m is the temperature of maximum reaction rate and can be obtained from a plot of α against T.

Different models have been proposed for solid state reactions depending on the type of processes leading to the reactions [29]. In the present case application of H–M relation leads to a good linear fit in the case of $f(\alpha) = (1 - \alpha)^{1/2}$, which suggests a contracting cylinder

TABLE V Results of decomposition process of $Di_2(C_4H_4O_6)_3 \cdot 5H_2O$

Stage	Decomposition temperature (°C)	Decomposition step	Observed mass loss (%)	Calculated mass loss (%)
1st stage	50 to 200	$Di_2(C_4H_4O_6)_3 \cdot 5H_2O \downarrow Di_2(C_4H_4O_6)_3$	11.50	10.98
2nd stage	235 to 360	$Di_2(C_4H_4O_6)_3 \downarrow Di_2(C_2O_4)_3$	32	32.96
3rd stage	380 to 490	$Di_2(C_2O_4)_3 \downarrow Di_2(CO_3)_3$	42	43.22
4th stage	490 to 760	$Di_2(CO_3)_3 \downarrow Di_2(O_3)$	57.5	59.34

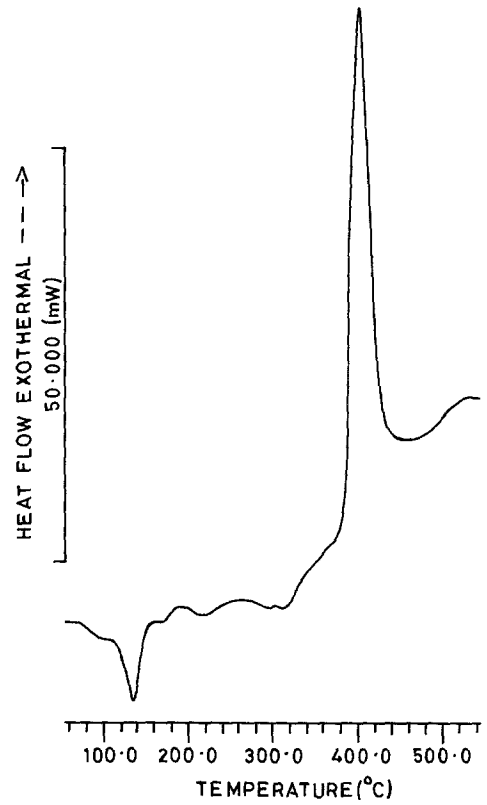

Figure 8 DSC curve recorded for $Di_2(C_4H_4O_6)_3 \cdot 5H_2O$.

kinetic model as the appropriate one for the mechanism of decomposition. The Coats–Redfern relation also gives a linear fit for $g(\alpha) = 2[1 - (1 - \alpha)^{1/2}]$ thereby confirming the application of same mechanism of decomposition. The kinetic parameters like activation energy E, order of reaction n and frequency factor Z as calculated from the first stage of decomposition are recorded in Table VI. The values as calculated on application of three kinetic equations (Table VI) are in reasonably good agreement. The complete agreement on the reaction mechanism responsible for the decomposition as obtained on application of C–R and H–M relations is noteworthy; both suggesting the contracting cylinder kinetic model as the relevant one for the explanation of results obtained in the present case.

4. Conclusions

1. The silica gel system involving the use of didymium nitrate as the upper reactant and sodium metasilicate gel impregnated with tartaric acid results into growth of didymium tartrate crystals.

2. X-ray and TEM studies reveal crystallinity of $Di_2(C_4H_4O_6)_3 \cdot 5H_2O$.

3. The chemical analysis coupled with the results of IR spectroscopy and thermogravimetric analysis establish the crystals to be hydrated with the stoichiometry $Di_2(C_4H_4O_6)_3 \cdot 5H_2O$. Qualitative elemental analysis (EDAX) shows presence of La and Nd in high concentrations while Pr and Sm are present in low concentrations.

4. The results of mass spectroscopy indicate the fragmentography of the material giving the base peak at $M/E = 18$. There is also a significant peak of tartrate ion at $M/E = 149$. There is a spontaneous change in the state of crystallinity of the material when examined under TEM. This change is attributed to electron beam heating and the presence of water molecules in the material.

TABLE VI Energy of activation, order of reaction and frequency factor calculated from 1st stage of decomposition

Relation used	Order of reaction, n	Frequency factor, Z	Energy of activation, E_a (kcal mol^{-1})*
Horowitz–Metzger [26]	$\frac{1}{2}$	–	13.745
Piloyan–Novikova [27]	–	2.61×10^5	5.354
Coats–Redfern [28]	$\frac{1}{2}$	6.11×10^5	13.748

*1 kcal = 4.187 kJ.

5. The thermal behaviour suggests the material to be unstable even at lower energies. The decomposition of the material starts at 50° C and after going through different intermediates, gets reduced to Di_2O_3 at 760° C.

6. Thermograms and DSC give a clear indication of the fact that all transformations are associated with mass changes. This rules out the possibility of any structural change during the process of decomposition.

7. Applications of H–M and C–R relations for the kinetic model reveal "contracting cylinder" as the most appropriate one for the explanation of solid state reactions involved in the decomposition process.

Acknowledgement

One of us (K. K. R.) is thankful to the University of Jammu for the award of research fellowship. The authors are thankful to Professor N. K. Rao, Head, Physics Department, Jammu University, Jammu for his encouragement.

References

1. M. SCHIEBER, A. GRILL and Y. AVIGAL, *J. Cryst. Growth* **13/14** (1972) 579.
2. M. SCHIEBER, A. GRILL and I. SHIDLOVSKY, *ibid.* **3/4** (1968) 467.
3. H. MAKINO, *Jpn. J. Appl. Phys.* **15** (1976) 415.
4. M. SCHIEBER and L. HOLMES, *J. Appl. Phys.* **35** (1964) 1004.
5. G. A. ANDREEV, *Soviet Phys-Solid State* **7** (1965) 140.
6. *Idem, Soviet Phys-Cryst.* **12** (1967) 82.
7. O. L. KREININ and K. M. ROZIN, *ibid.* **18** (1973) 276.
8. B. JOUKOFF and A. M. JEAN-LOUIS, *J. Cryst. Growth* **12** (1972) 169.
9. M. SCHIEBER, *J. Amer. Ceram. Soc. Bull.* **40** (1961) 563.
10. A. I. AGRANOVSAKAYA and YU. G. SAKSONOV, *Soviet Phys. Cryst.* **11** (1966) 196.
11. E. A. VINOGRADOV and L. K. VODOP'YANOV, *Soviet Phys.-Solid State* **17** (1975) 2088.
12. A. R. PATEL and S. K. ARORA, *J. Cryst. Growth* **37** (1977) 343.
13. *Idem, Kristall Und Technik* **13** (1978) 899.
14. *Idem, ibid.* **13** (1978) 1445.
15. B. WIKTOROWSKA, B. BORECKA and J. KARNIEWICZ, *J. Mater. Sci.* **18** (1983) 416.
16. G. A. KIOSSE, in "Crystal Structure of Inorganic Compounds" edited by T. I. Malinowskii (Shtuntsa, Press, Kishineve 1974) p. 103, in Russian.
17. P. N. KOTRU, N. K. GUPTA, K. K. RAINA and I. B. SHARMA, *J. Mater. Sci.* **21** (1986) 83.
18. P. N. KOTRU, N. K. GUPTA, K. K. RAINA and

M. L. KOUL, *Bull. Mater. Sci.*, in press.
19. P. N. KOTRU, K. K. RAINA and M. L. KOUL, Soviet Phys. Cryst. (Russia), in press.
20. P. N. KOTRU, N. K. GUPTA and K. K. RAINA, *Kristall Technik* **21** (1986) 15.
21. *Idem, J. Mater. Sci.* **21** (1986) 90.
22. P. N. KOTRU, K. K. RAINA and N. K. GUPTA, *Kristall Technik*, in press.
23. P. N. KOTRU and K. K. RAINA, *J. Mater. Sci. Lett.*, in press.
24. M. H. LORETTO, in "Physico-Chemical Methods of Mineral Analysis", edited by A. W. Nicol (Plenum Press, New York, 1975).
25. C. ALFERD, G. LATZ, I. LITANT and B. RUBIN, "Analytical Calorimetry". Vol. 2, (Plenum Press, New York, 1970) p. 255.
26. H. H. HOROWITZ and G. METZGER, *Anal. Chem.* **35** (1963) 1464.
27. G. P. PILOYAN and O. S. NOVIKOVA, *Russian J. Inorg. Chem.* **12** (1966) 313.
28. A. W. COATS and J. P. REDFERN, *Nature* **201** (1964) 68.
29. SESTAK in "Thermal Analysis", Proceedings of the 3rd International Conference on Thermal Analysis, edited by Wiedemann, Vol. 2 (1971) p. 24.

Received 26 September 1985
and accepted 21 January 1986